

Development and Evaluation of Superporous Ceramics Bone Tissue Scaffold Materials with Triple Pore Structure A) Hydroxyapatite, B) Beta-Tricalcium Phosphate

Michiko Sakamoto and Toshio Matsumoto
*R&D Department PENTAX New Ceramics Division HOYA Corporation
Japan*

1. Introduction

Hydroxyapatite ceramics (HAp) have been used as bone graft materials, due to their excellent biocompatibility and osteoconductivity. Moreover, they had a wide range of porosity for using various bone defect parts. For example, HAp from 0 to 15 % porosity with high strength was useful as an ilium spacer, intervertebral spacer which requires high strength. HAp from 30 to 40% porosity was useful as spinous process spacer for laminoplasty which requires bone formation and middle strength. Furthermore, HAp from 40 to 60% porosity was useful for the calvarias plate which requires good bone formation (Fig.1). However, due to the mechanical strength, the porosity was limited to 60% or less. Recently, regenerative therapy using cellular activity to cure bone defects has been developed, requiring HAp with porous spaces which cells can populate. We have developed superporous HAp (HAp-S) and designed the porosity, pore size and pore structure of HAp-S for managing directly-opposing factors of both high porosity and mechanical strength. In this study, the properties of HAp-S were examined in vitro using primary rat calvarial osteoblasts culture and an implant model using the canine femoral defect model, ilium defect model and rat calvarial defect model.

Moreover, we report on Beta-tricalcium phosphate (Beta-TCP) ceramics, which have been used as bone tissue scaffold like HAp. Since 1999 in Japan, Beta-TCP ceramics have also been widely used as bone tissue scaffold materials in many areas of surgery due to their biocompatibility and biodegradation. Beta-TCP is gradually degraded in the bone tissue and replaced with natural bone. However, if the degradation rate is faster than the bone formation rate, the mechanical strength of Beta-TCP may become poor in the bone tissue. This study evaluated the degree of osteointegration of superporous Beta-TCP ceramics (TCP-S) with the same high porosity and triple pore structure as HAp-S (Apaceram -AX). In our previous study, HAp-S, which has smaller pores in HAp-Ss artificial bone made by two types of surfactants, was most suitable as an artificial bone. However, biodegradation of TCP is different in characteristics from non-biodegradation. We investigated whether the most suitable parameter of HAp applies to TCP using a canine femoral defect model (short term). The most suitable TCP was then selected as an artificial bone and the long-term

osseous implantation test, biomechanical examination and the micro-CT measurement were evaluated.

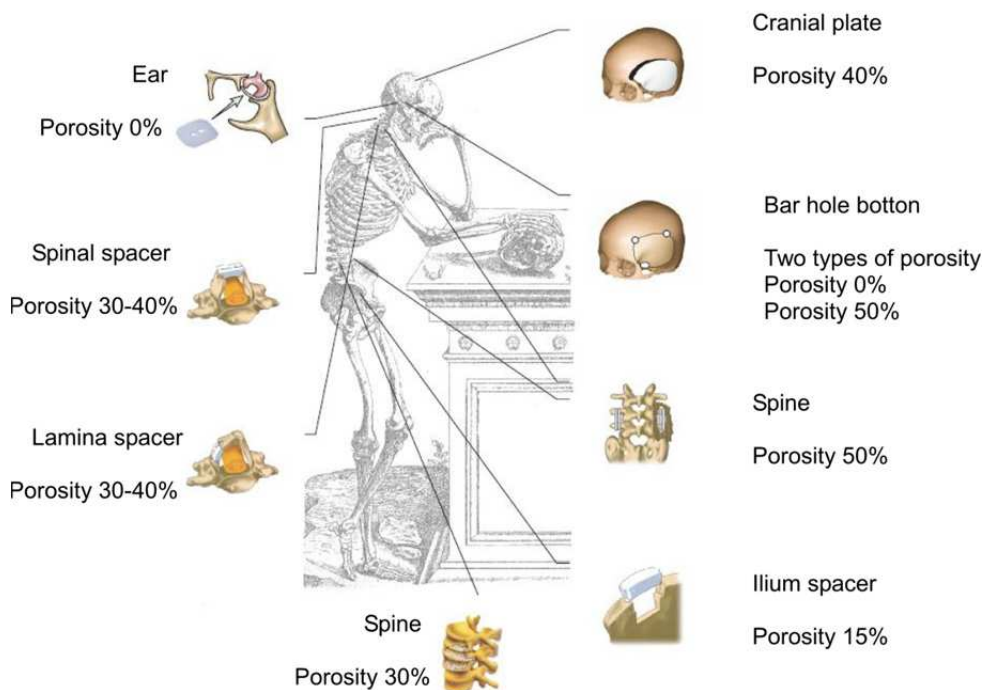


Fig. 1. Schematic drawing presenting the potential usage of HAp in various degrees of porosity. HAp from 0 to 15 % porosity with high strength was useful as an ilium spacer, intervertebral spacer which requires high strength. HAp from 30 to 40% porosity was useful as spinous process spacer for laminoplasty which requires bone formation and middle strength. Furthermore, HAp from 40 to 60% porosity was useful for the calvarial plates which require good bone formation.

A) Superporous hydroxyapatite ceramics

2. Material and methods

2.1 Formation of superporous hydroxyapatite

An aqueous solution of phosphoric acid was poured into a suspension of purified calcium hydroxide, which resulted in hydroxyapatite slurry. The slurry was sprayed and dried using the spray-dry method to produce a fine spheroid powder. HAp powder was homogenized in water. A water soluble polymer was added to the slurry as a binder. A surfactant was used for bubble formation and micro air bubbles were introduced into the HAp slurry. The slurry was gelated and dried. The green block was then shaped into a disk and rod and sintered at 1200°C in air.

2.2 Measurement of compression strength

The compression strength of the HAp-S and HAp50 were measured by the recommended method of JIS at the speed of 0.5 mm/min by Autograph DSS (Autograph DSS/5000, Shimadzu Co., Kyoto, Japan).

2.3 Scanning Electron Microscopy (SEM) observation

The surface and inside structures of HAp-S and HAp50 were observed by SEM (S-4200, Hitachi Co., Tokyo, Japan).

2.4 In vivo: Animal test

2.4.1 Canine femoral defect model

HAp-S 4 mm in diameter and 12 mm in length was implanted at 2 sites in the left and right femurs of three male beagle dogs following ISO10993-6. Four weeks after implantation, animals were euthanized and the left and right femurs of three beagles were dissected out, and the effects and changes in the surrounding tissue and implanted material were histologically examined using Toluidine Blue (T.B) staining. The comparative material was HAp with 50% Porosity (HAp-50).

2.4.2 Canine ilium defect model (biomechanical testing)

HAp-S 4 mm in diameter and 6 mm in length was implanted at 1 site in the ilium of male beagles for 4 following ISO10993-6. Four weeks and 13 weeks after implantation, the ilium of 3 beagles was excised. The operative segments were gently trimmed off all the soft tissue. Before biomechanical testing, each specimen was fixed using resin. They were evaluated by nondestructive compression strength testing (until compressed 0.5mm by adding load) using a biomechanical testing machine (858 Mini Bionix II, MTS System Co., Minneapolis, MN, USA). Moreover, the effect and change of HAp-S were investigated histologically by T.B staining.

2.4.3 Rat calvarial defect model

The periosteum of the calvaria of Wistar rats was removed, and in the calvaria, defects measuring 4 mm in diameter and 1 mm in depth were made. HAp-S matching the defect in size was implanted and the periosteum was replaced. 12 weeks after implantation, the calvarias of 3 rats were excised, and the effects and changes in the surrounding tissue and implanted material were histologically investigated..HAp-50 was used as control material porosity 50%.

2.5 In vitro

Newborn Wistar rats were sacrificed by chloroform and their calvarias were removed aseptically. They were minced, washed with PBS, and digested by a 0.1% collagenase solution in a digestion chamber at 37°C for 90 min. They were filleted with a cell strainer and the filtrates were centrifuged at 1000 rpm for 5 min. The osteoblasts were suspended in 10 ml of MEM containing 100 U/mL penicillin, 100 µg/mL streptomycin, 0.25µg/mL fungison, and

15% FBS. The cell number was counted and adjusted to 7×10^5 counts of osteoblasts / pellet. The osteoblasts were laid on HAp-S and HAp-50% pellets. They were incubated in the culture medium described earlier at 37°C in a CO₂ incubator. The pellets of 3, 7 and 14 days of culture were estimated by alkaline phosphatase activity and ALP staining.

2.5.1 Alkaline phosphatase (ALP) activity

The pellets with the cells were washed with PBS, crushed by a cryo-press, and transferred into tubes. Five hundred μ L of 10% Triton-X 100 aqueous solution, and 250 μ L of 2-1-amino-2-methyl-1-propanol buffer were added, followed by the addition of 250 μ L of substrate. The mixture was kept at 37°C for 15 min. The reaction was stopped with 250 μ L of 1N NaOH, and the absorbance was measured at 450 nm.

2.5.2 ALP staining

The pellets with the cells were washed with PBS, fixed for 30 s with a 60% acetone-citrate buffer, washed with distilled water for 45 s, and reacted with a dye mixture for 30 min in the dark. The dye mixture was composed of 48 mL of a fast violet B salt solution and 2 mL of a 0.25% naphthol AS-MX phosphate alkaline solution. After the reaction, the pellets were washed with distilled water and photographed using a digital surface microscope.

3. Results

3.1 Characteristics of superporous hydroxyapatites

The porosity of HAp-S measured by its volume density was 85%. The porosity was the highest among the inorganic ceramics as bone substitute material. The compression strength of HAp-S was approximately 2 MPa which is manageable during surgery (Table 1).

Sample name	HAp-S	HAp-50
General name	Hydroxyapatite	Hydroxyapatite
Molecular formula	$\text{Ca}_{10}(\text{PO}_4)_6(\text{OH})_2$	$\text{Ca}_{10}(\text{PO}_4)_6(\text{OH})_2$
Porosity	85%	50%
Pore structure	Consist of Spherical macro pore and micro pore	
Macro pore	50~300 μ m	50~500 μ m
Interconnected pore	50~100 μ m	—
Micro pore	0.5~10 μ m	0.5~10 μ m
Compression strength	2.0MPa	30.0MPa

Table 1. Characteristic of HAp-S and HAp-50.

3.2 SEM observation

In HAp-S, the size of the macro pores was from approximately 50 to 300 μ m (Table 1). Under high magnification, there were many interconnecting pores among the macro pores and micro pore gaps between secondary particles of HAp ceramics on the pore walls. The size of the interconnecting pores and micro pores was from 50 to 100 μ m, and from 0.5 to 10 μ m, respectively (Table 1). In brief, HAp-S had the triple pore structure (Fig.2 a,b).

In HAp-50, the size of the macro pores averaged between 50 and 500 μm (Table 1). There were micro pore gaps between secondary particles of HAp ceramics on the pore walls. The size of the micro pores varied from 0.5 to 10 μm . HAp-50 had the interconnecting pore structure with the macro pores and micro pores (Fig.2 c) and d)).

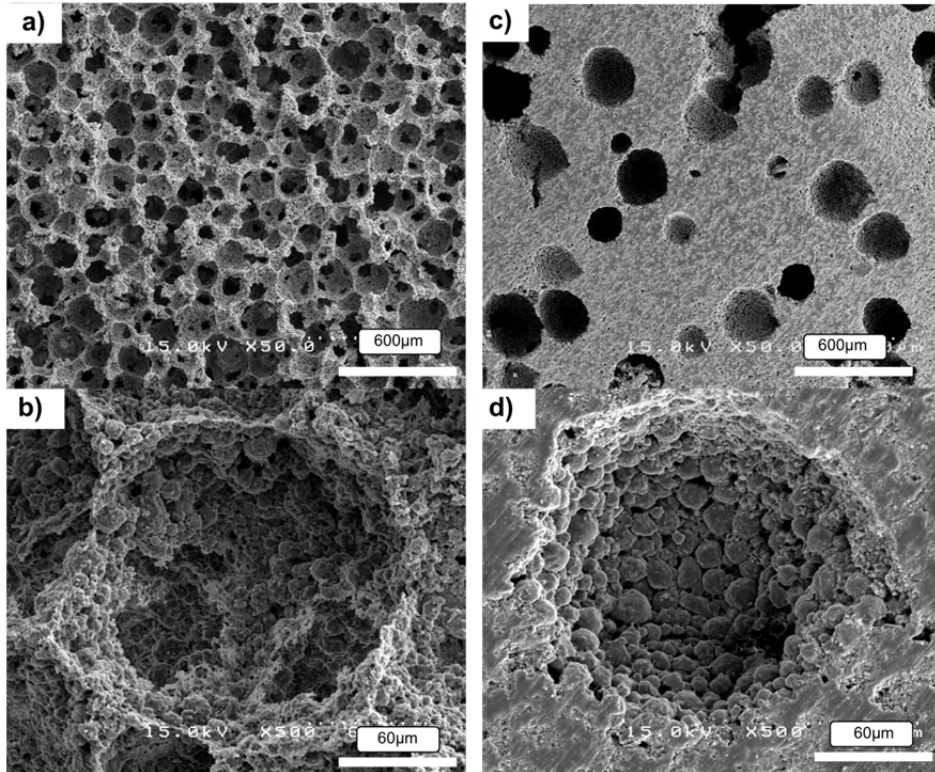


Fig. 2. SEM images of HAp-S a) b) and HAp-50 c),d). a), c): $\times 50$ b), d): $\times 500$
a): The size of the macro pores was from approximately 50 to 300 μm .
b): There are many interconnecting pores among the macro pores and micro pore gaps between secondary particles of HAp ceramics on the pore walls. The size of the interconnecting pores and micro pores is from 50 to 100 μm , and from 0.5 to 10 μm , respectively. HAp-S had the triple pore structure.
c): The size of the macro pores was from approximately 50 to 500 μm .
d): There are micro pore gaps between secondary particles of HAp ceramics on the pore walls. The size of the micro pores is from 0.5 to 10 μm .
HAp-50 had the interconnecting pore structure with the macro pores and micro pores.

3.3 In vivo animal test

3.3.1 Canine femoral defect model

T.B staining in HAp-S 4 weeks after implantation showed new bone formation in the entire implanted material area (Fig.3). Moreover, tissue of the surrounding implanted area did not

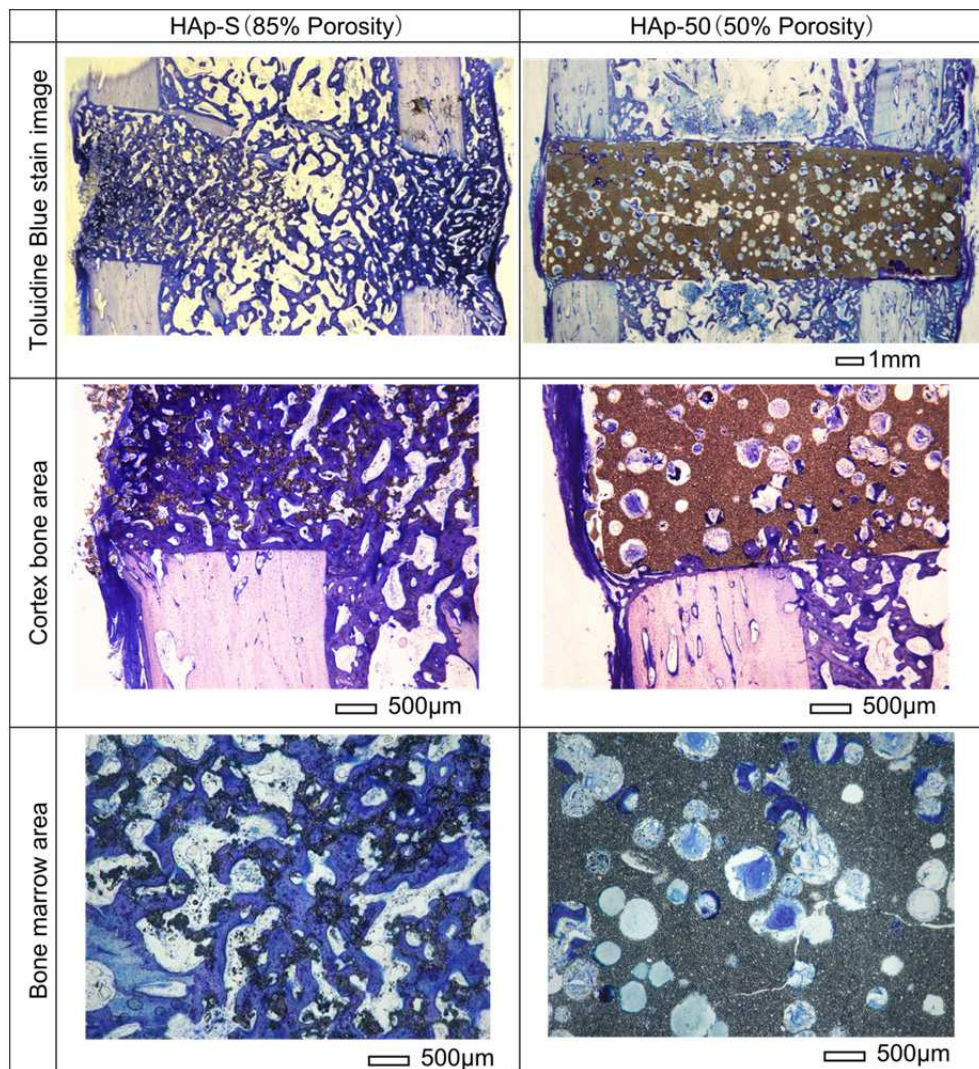


Fig. 3. T.B staining of femur of beagle at after 4 weeks implanted.

T.B staining in HAp-S 4 weeks after implantation showed new bone formation in the entire implanted material area. Moreover, tissue of the surrounding implanted area did not show any abnormalities. The magnified image of the cortex in HAp-S showed new bone formation not only in the boundary area between the original cortex bones, but also inside HAp-S. On the other hand, although T.B staining of HAp-50 showed new bone formation in the surrounding material and pores on the surface, new bone formation was not observed in the pores inside the material.

show any abnormalities. The magnified image of the cortex in HAp-S showed new bone formation not only in the boundary area between the original cortex bones, but also inside HAp-S. On the other hand, although T.B staining of the comparative material HAp-50 showed new bone formation in the surrounding material and pores on the surface, new bone formation was not observed in the pores inside the material. T.B staining in HAp-S 4 weeks after implantation showed new bone formation in the entire implanted material area. Moreover, tissue of the surrounding implanted area did not show any abnormalities.

The magnified image of the cortex in HAp-S showed new bone formation not only in the boundary area between the original cortex bones, but also inside HAp-S. On the other hand, although T.B staining of HAp-50 showed new bone formation in the surrounding material and pores on the surface, new bone formation was not observed in the pores inside the material.

3.3.2 Canine ilium defect model (biomechanical testing)

The compression strength of the HAp-S 4 weeks after implantation was 6-fold higher than that before implantation. Thirteen weeks after implantation, the compression strength of the HAp-S was over 8-fold higher than that before implantation. The strength of the bone defect was recovered at the early stage with the period of implantation (Fig.4-1). T.B staining of HAp-S showed the HAp-S material surrounding new bone formation tissue (Fig.4-2). Moreover, because the formation of bone tissue among the inside materials was tightly bonded by the micro pores of HAp-S.

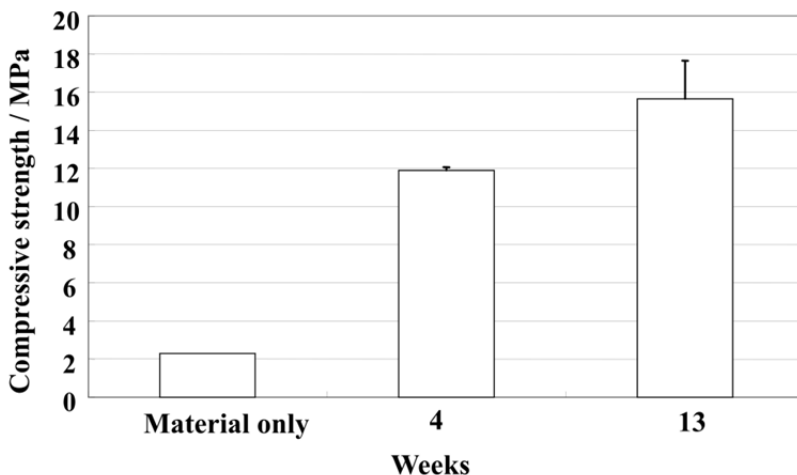


Fig. 4-1. Time course of Compressive strength of HAp-S after implanted.

The compression strength of the HAp-S 4 weeks and 13 weeks after implantation was 6-fold and 8-fold higher than that before implantation. The strength of the defect recovered at the early stage with the period of implantation.

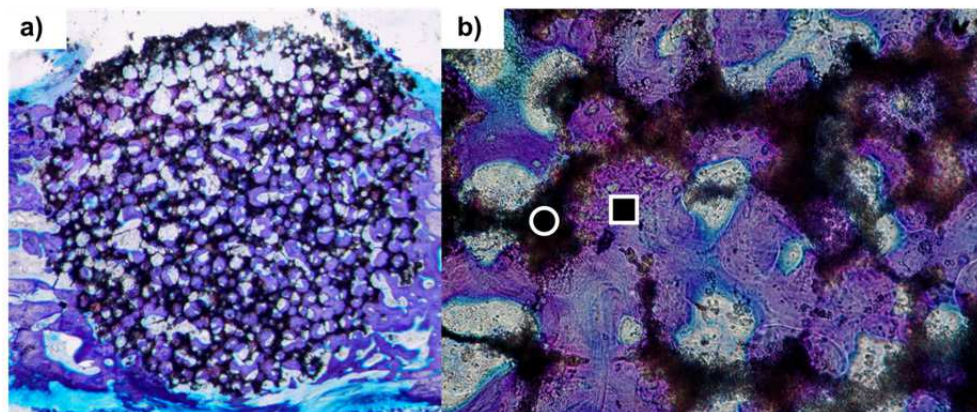


Fig. 4-2. TB staining of ilium of beagle at after 4 weeks implanted.

a) Whole image of HAp-S b) Enlarged image of a) ○ : HAp-S □: New bone
Some part of HAp-S particles was surrounded by newly formed bone closely.

3.3.3 Rat calvarial defect model

H.E staining of HAp-S showed that the HAp-S material had excellent new bone formation tissue not only in the surrounding area, but also the entire HAp-S area. Moreover, tissue surrounding the implanted area did not show any abnormalities. On the other hand, H.E staining of the comparative material HAp-50 showed new bone formation in the surrounding material (Fig.5).

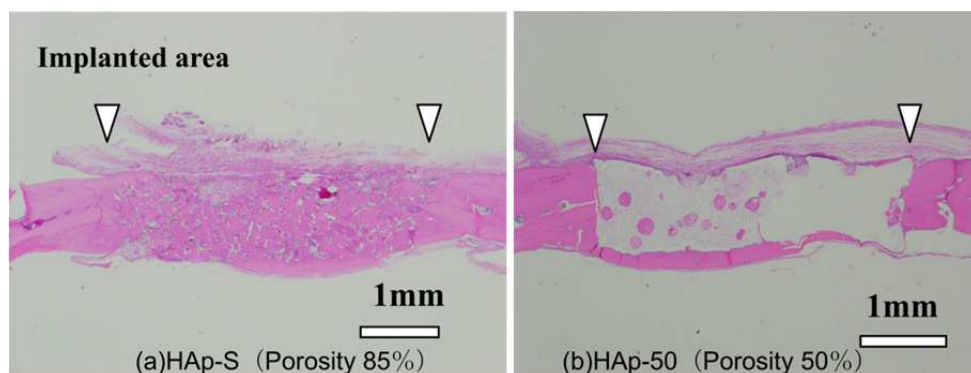


Fig. 5. HE staining of calvaria of rat at after 12 weeks implanted.

a) HE staining of HAp-S showed that the HAp-S material had excellent new bone formation tissue not only in the surrounding area, but also the entire HAp-S area.
b) HE staining of the comparative material HAp-50 showed new bone formation in the surrounding material.

3.4 In vitro test

ALP activity of HAp-S was higher than that of HAp-50 during the entire culture period (Fig.6-1). ALP staining of HAp-S was showed staining on the surface and inside of HAp-S. In contrast, ALP staining of HAp-50 was showed on the upper surface.(Fig.6-2)

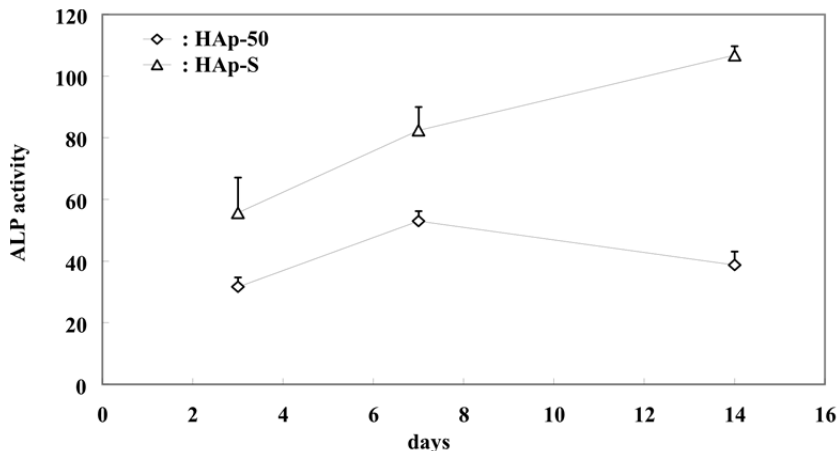


Fig. 6-1. Time course of ALP activities. \triangle : HAp-S \diamond : HAp-50
 ALP activity of HAp-S is higher than that of HAp-50 during the entire culture period.

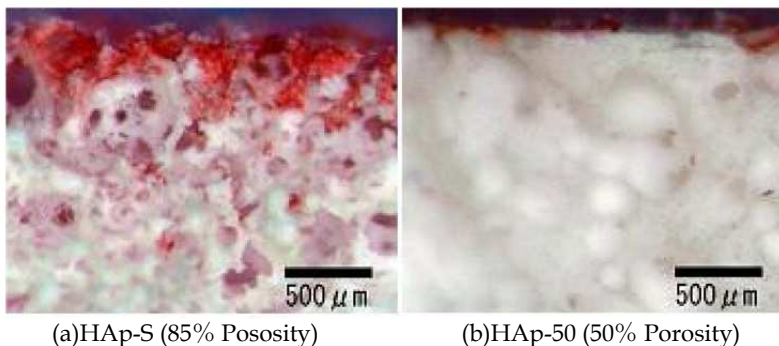


Fig. 6-2. ALP staining of sectioned sample at 14days after seeding.
 ALP staining of HAp-S showed staining on the surface and inside of HAp-S. In contrast, ALP staining of HAp-50 showed that only the surface.

4. Discussion

Recently, regenerative therapy using cellular activity to cure bone defects has been developed. Cellular activity required HAp with porous spaces that allows cellular penetration in order to obtain the most suitable porosity, optimal pore size and favorable pore structure, we considered the following aspects:

1. Porosity: We reviewed materials and facilities requiring the addition of a bubble method. In the conventional method, bubble formation is created by mixing and naturally adding air to the slurry. This time, we added surfactant and formed unprecedented micro bubbles in the HAp slurry.
2. Pore size: Adding surfactant allowed uniformity of the macro pores and interconnecting pores. If these pore sizes are too large, the inside of pores will be covered with fibrous tissue. As a result, bone formation was prevented by fibrous tissue. If these pore sizes are too small, cell cannot permeate to the inside of the materials and bone formation will be limited to the surface layer. Therefore, determining the ideal pore size was required for good bone formation. We chose the surfactant which created more uniform micro bubbles. Moreover, it was important to keep adding bubbles to the slurry without crushing until the final shape was obtained.
3. Pore structure: To present a scaffold that is necessary for more excellent bone formation, we investigated the condition of HAp powder and achieved porosity of the pore structure. Macro pores were necessary to provide a comfortable space for cells to penetrate. Interconnecting pores were required to allow penetration to the inside of HAp. Micro pores were required as the super bonding space for cells (Fig.7).

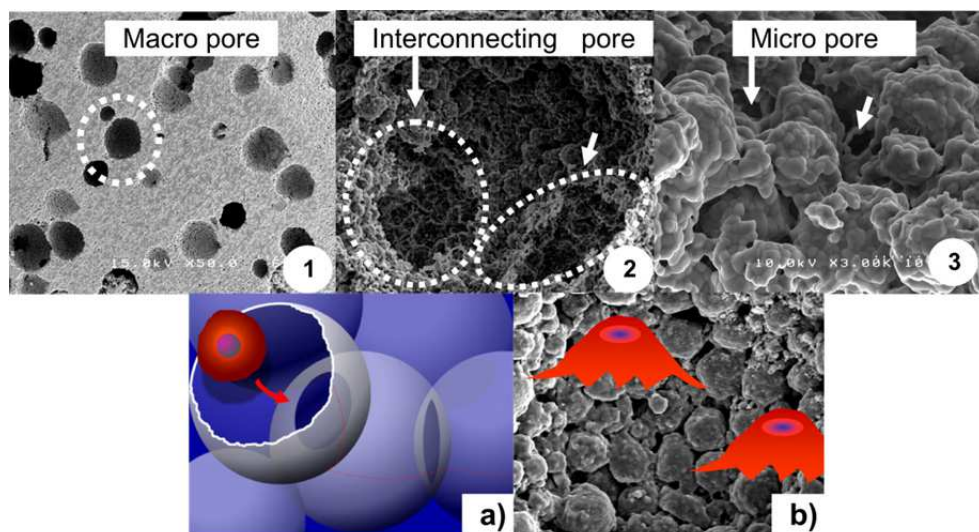


Fig. 7. Images 1,2,3) & illustrations a,b) of triple pore structure

- 1: Macro pores were necessary to provide a comfortable space for cells to penetrate.
- 2: Interconnecting pores were required to allow penetration to the inside of HAp(a).
- 3: Micro pores were required as the super bonding space for cells (b).

In the above improvements, the porosity of HAp-S was 85%, and its compression strength was approximately 2.0MPa. Although the porosity of HAp-S was the highest among the commercial inorganic ceramics artificial bones, mechanical property was enough during surgery. In the *in vivo* test, HAp-S had better new bone formation tissue in not only the surrounding area, but also the entire area of HAp-S than that of HAp-50. Moreover, HAp-S

showed regenerative bone tissue, integration with the surrounding tissue and recovery of the compression strength of the defect area in the early stage. These results strongly suggest that the controlled triple pore structure, namely, uniform macro pores, many interconnecting pores and micro pores on the pore wall, advances osteogenesis.

5. Conclusion

HAp-S was confirmed to have the most suitable pore structure for bone regeneration as the bone substitute material, and as being a useful material for application to bone disease.

In 2006, HAp-S (APACERAM-AX, HOYA Co., Tokyo, Japan) was approved by the MHLW as a bone substitute in orthopedics for spine fusion and tumors, as well as the dental field. The clinical data on the follow-up more than 5 year after the treatment with HAp-S showed favorable results in all cases.

B) Superporous Beta-tricalcium phosphate ceramics

6. Materials and method

6.1 Formation of superporous Beta-tricalcium phosphate (TCP-S)

Beta-TCP powder was made by wet mixing and the spray-dry method. Beta-TCP powder was homogenized in water. A water soluble polymer was added to the slurry as binder. Two types of surfactant were used to form inner pores. One was anionic (AN), and the other was nonionic (NI). The surfactant was used as bubbled formation in the Beta-TCP slurry, which was gelated and dried. The dried block was shaped into blocks and rods and, then sintered at 1,100°C in air.

Sample name	TCP-S(AN)	TCP-S(NI)
General name	Beta-tricalcium phosphate	Beta-tricalcium phosphate
Molecular formula	$\text{Ca}_3(\text{PO}_4)_2$	$\text{Ca}_3(\text{PO}_4)_2$
Porosity	75%	75%
Pore structure	Consist of Spherical macro pore and micro pore	
Macro pore	50~300 μm	50~500 μm
Interconnected pore	50~100 μm	50~100 μm
Micro pore	0.5~10 μm	0.5~10 μm
Compression strength	6.0MPa	5.0MPa

Table 2. Characteristics of TCP-S(AN) and TCP-S(NI)

6.2 Measurement of compression strength

The compressive strength of two types of TCP-Ss was measured at 1 mm/min of test speed by Autograph AGS-H (SHIMADZU Co., Kyoto, Japan). The test sample was 10×10×20 mm in size.

6.3 SEM observation

The surface and inner structures of TCP-Ss were observed by SEM (S-4200, Hitachi Co., Tokyo, Japan).

6.4 Animal experiments

6.4.1 Canine femoral defect model (short term)

Adult beagles weighing 10~13 kg were used. After anesthetization, the integument and fascia of the femur were incised using an electrical surgical knife. Holes were drilled in both femora of beagles 4 mm in diameter and 12 mm in depth according to the implant shape and two types of TCP-Ss were implanted in each hole. The hole positions were approximately 40 mm (distal position) and 60 or 70 mm (proximal position) from the apophysis of the femur. At 1, 2 and 3 weeks postoperatively, the femora were harvested. A T.B. staining specimen was prepared and the histopathology examined.

6.4.2 Canine femoral defect model (long term)

Adult beagles weighing 10~13 kg were used. After anesthetization, the integument and fascia of the femur were incised using an electrical surgical knife. Holes were drilled in both femora of beagles 4 mm in diameter and 12 mm in depth according to the implant shape and TCP-Ss were implanted in each hole. The hole positions were approximately 40 mm (distal position) and 60 or 70 mm (proximal position) from the apophysis of the femur. For the 26-week implantation test, we used very small markers made of dense Hydroxyapatite 0.8 mm in diameter and 3.5 mm in length. The marker was implanted 55 mm from the apophysis of the femur. At 2, 4, 13 and 26 weeks postoperatively, the femora were harvested. T.B. staining specimens were prepared and the histopathology examined.

6.4.3 Canine femoral defect model (biomechanical testing)

We tested the change in compressive strength of TCP-S after implantation 2, 4 and 8 weeks postoperatively in the same beagle model. The sample for the compressive strength test was trimmed to 12 mm in length. Then, the compressive strength of the materials was analyzed using 858Mini Bionix (MTS, cross head speed 0.5 mm/min, destructive test, displacement about -1.5~2.0 mm). The animal experiment was in conformity with ISO10993-6:2007.

6.4.4 Rat calvarial defect model (micro-CT measurement)

After the periosteum was removed, a defect 4 mm in diameter and 1 mm in length was made in the calvarias of Wistar rats. Then, TCP-S the same size as the defect was implanted and the periosteum was returned. Four weeks after implantation, the calvarias of 3 rats were excised and scanned by micro-CT (Skyscan1172, SKYSCAN Co., Kontich, Belgium). The ratio of bone formation and absorption of material in TCP-S was calculated.

7. Result

7.1 Characteristics of superporous TCP

The compressive strength of AN of TCP-S 10x10x20 mm in size was approximately 6 MPa at 75% porosity and that of NI of TCP-S 10x10x20 mm in size was approximately 5 MPa at 75% porosity, respectively. The uniform pore structures gave a compressive strength higher than other commercial products with the same composition and porosity. This compressive strength had been strong enough to handle.

7.2 SEM observation

The porosity of these materials is about 75%. The pore size of AN of TCP-S is approximately 200 μm and that of NI of TCP-S is approximately 300 μm . The macro pores of both were very uniform. Moreover, the two types of TCP-Ss had many interconnecting pores and micro pores on the pore wall (Fig.8). Both TCP-Ss had a uniform triple pore structure with 75% porosity.

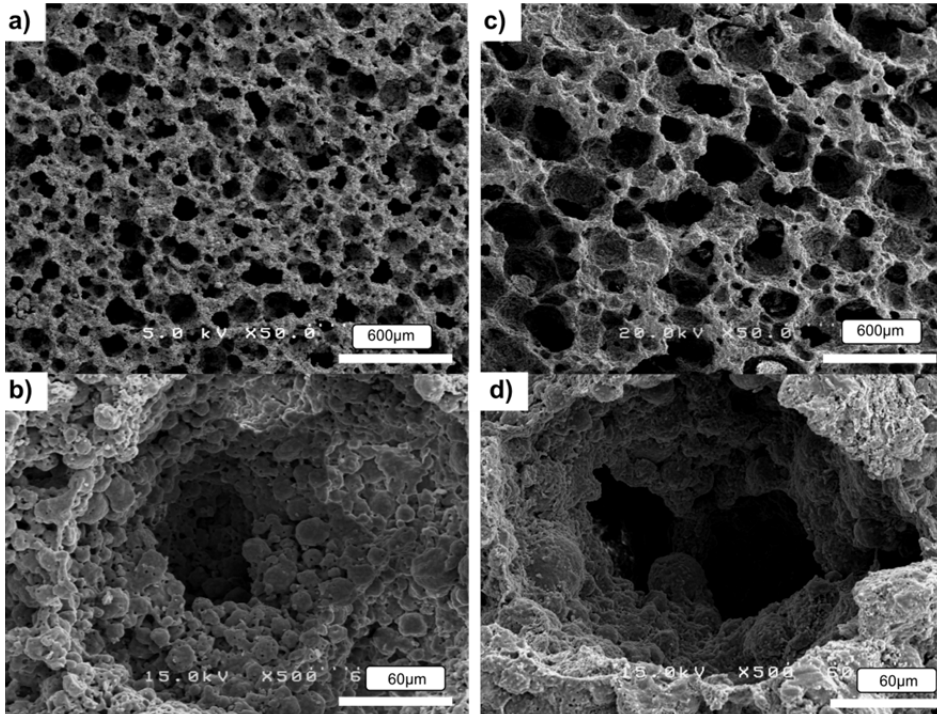


Fig. 8. SEM images of TCP(AN) and TCP(NI).

a), b): TCP(AN) c), d): TCP(NI) a), c): $\times 50$ b), d): $\times 500$

a): The size of the macro pores was from approximately 50 to 500 μm .

c): The size of the macro pores was from approximately 50 to 300 μm .

b), d): There are many interconnecting pores among the macro pores and micro pore gaps between secondary particles of TCP ceramics on the pore walls. The size of the interconnecting pores and micro pores is from 50 to 100 μm , and from 0.5 to 10 μm , respectively. TCP-S(AN) and TCP-S(NI) had the triple pore structure.

7.3 Animal experiments

7.3.1 Canine femoral defect model (short term)

At 1 week postoperatively, moderate proliferation of the periosteum was observed at the outer femur surface of AN and NI of TCP-Ss. New bone was not observed in either material. At 2 weeks postoperatively, the AN specimen showed new bone not only at the area adjacent to the

cortex bone but also the inner pores of the specimen. In contrast, although the NI specimen showed new bone at the area adjacent to the cortex bone, new bone was observed only slightly inside the specimen. At 3 weeks postoperatively, new bone formation on both specimens was better than that at 2 weeks. The AN specimen showed better early bone formation, and in an extended image, some parts of the TCP-S particles were closely surrounded by newly formed bone. On the other hand, the NI specimen showed that there was a gap between the material and new bone tissue (Fig. 9 and 10). The TCP-S of AN showed just TCP-S.

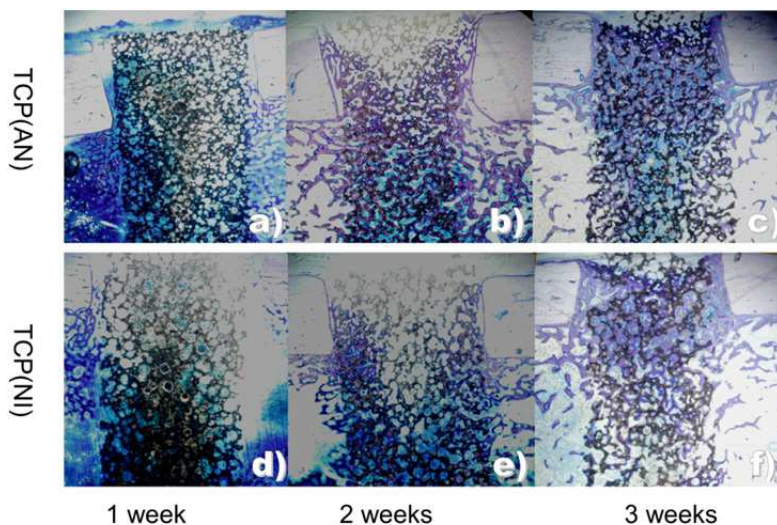


Fig. 9. T.B staining of femur of beagle at after 1,2 and 3 weeks implanted.

a), b),c): TCP(AN) d),e),f): TCP(NI)

a), d):1week b),e):2weeks c),f):3weeks

At 1 week postoperatively, moderate proliferation of the periosteum was observed at the outer femur surface of AN and NI of TCP-Ss. At 2 weeks postoperatively, the AN specimen showed new bone not only at the area adjacent to the cortex bone but also the inner pores of the specimen. In contrast, although the NI specimen showed new bone at the area adjacent to the cortex bone, new bone was observed only slightly inside the specimen. At 3 weeks postoperatively, new bone formation on both specimens was better than that at 2 weeks.

7.3.2 Canine femoral defect model (long term)

At 2 weeks postoperatively, osteoblasts and osteoclasts increased in number. The TCP-S specimen showed newly formed bone not only at the area adjacent to the cortex bone but also the inner pores of TCP-S. The triple pore structure of TCP-S was suitable for penetrating into the inner pores for fibrous tissue, bone tissue and so forth at the very early stage. At 4 weeks postoperatively, newly formed bone was expressed better than that at 2 weeks, especially in the cortex bone. Remnant TCP-S in the cortex bone and medullar was slight. Some parts of the TCP-S particles were closely surrounded by the newly formed bone. This result depended on the controlled triple pore structure, namely macro pores, interconnecting pores and micro pores, and each pore size of TCP-S. At 13 weeks postoperatively, osteoblast and osteoclast

further increased in number greater than that of 4 weeks. Newly formed bone in the cortex bone was more mature than in the medullar. Moreover, the mature bone tissue in the cortex bone showed the same lamellar pattern as natural bone. Remnant TCP-S in the cortex bone and medullar was much less than that of 4 weeks (Fig. 11). At 26 weeks, TCP-S implanted in

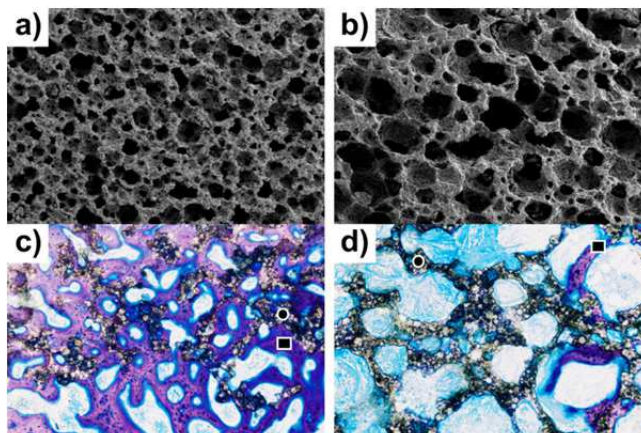


Fig. 10. SEM images of TCP-Ss and T.B staining of femur of beagle at after 3 weeks implanted. a), c): TCP(AN) b),d): TCP(NI)

a), b):SEM image

c), d): T.B. staining(Enlarged image of Fig.9-c and 9-f) ○ : TCP-S □ : New bone

The AN specimen showed better early bone formation, and in an extended image, some parts of the TCP-S particles were closely surrounded by newly formed bone. On the other hand, the NI specimen showed that there was a gap between the material and new bone tissue.

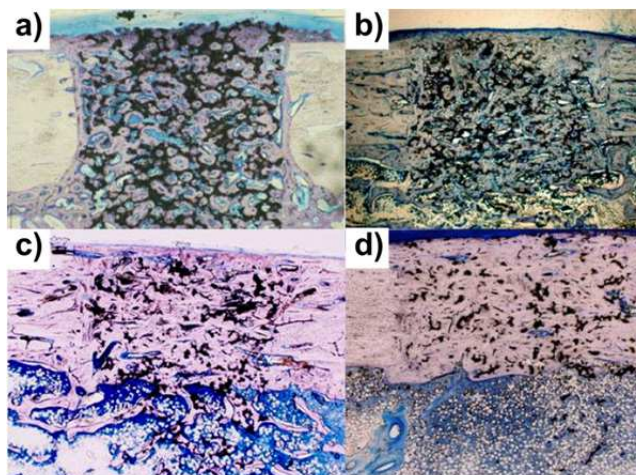


Fig. 11. T.B staining of femur of beagle at after 4,8,13 and 26 weeks implanted.

a): 4 weeks b): 8 weeks c): 13 weeks d): 26 weeks

At 4 weeks postoperatively, newly formed bone was expressed better than that at 2 weeks,

especially in the cortex bone. At 13 weeks postoperatively, newly formed bone in the cortex bone was more mature than in the medullar. At 26 weeks, TCP-S implanted in the cortex changed to cortex bone completely and that in the medullar changed to medullar completely, respectively.

the cortex changed to cortex bone completely and that in the medullar changed to medullar completely, respectively. Remnant TCP-S in the cortex bone was scarcely observed and remnant TCP-S in the medullar was not observed. TCP-S was gradually degraded in the bone tissue and replaced with natural bone completely at 26 weeks. These results of the animal study suggest that TCP-S with a triple pore structure had good osteogenesis and bioresorption in the early stage after implantation.

7.3.3 Femoral defect model (biomechanical testing)

The compressive strength of TCP-S in the distal position at 2, 4 and 8 weeks postoperatively was 40.2 MPa, 71.2 MPa and 81.7 MPa, respectively. On the other hand, in the proximal position, the compressive strength of TCP-S at 2, 4 and 8 weeks postoperatively was 36.2 MPa, 82.7 MPa and 89.7 MPa, respectively (Fig. 3). The compressive strength at 2 weeks increased approximately 8 times more than that of the material only. Moreover, during 4 and 8 weeks postoperatively, the compressive strength increased approximately 16 times more than that of the material only. The compressive strength of TCP-S implanted in defect bone was much higher than the material strength in the early stage. This result suggests that TCP-S showed early recovery of strength at the bone defect.

7.3.4 Rat calvarial defect model (micro-CT measurement)

In the Micro-CT image of 4 weeks after implantation, excellent bone formation in the TCP-S pellet was exhibited from the surroundings of the original bone. Moreover, Micro-CT analysis revealed that the ratio of bone formation was more than 50% in implantation at 4 weeks. In addition, the absorption of TCP materials was mean 3.9% with the ratio of absorbent material TCP-S. In the results of rat, at 4 weeks after implantation, the ratio of new bone formation in the TCP-S was higher than the materials absorption.

8. Discussion

Artificial bone consisting of HAp that was manufactured in Japan from about 1985, and artificial bone consisting of β -TCP featuring substitution of absorption bone that was not present in HAp manufactured from about 1999 have attracted attention. We investigated whether the most suitable parameter of HAp applies to TCP from the following aspects.

1. Pore size: In the absorption material of TCP-S, the bone formation in materials having a macropore greater than 300 μm produced a gap between the materials and new bone formation tissue. This is considered due to fibrous tissue entering and inhibiting bone formation. Materials and the new bone contacted closely, and the materials that had macropores less than 300 μm showed good bone formation. Regardless of the material properties, pore structure and pore sizes suitable for bone formation has been found to be common.

2. Strength recovery of the filling department: If the degradation rate is faster than the bone formation rate, the mechanical strength of Beta-TCP may become poor in the bone tissue. TCP-S with a triple pore structure showed that the compressive strength of TCP-S implanted in defect bone was much higher than the material strength in the early stage, because TCP-S was uniform and had the most suitable size and pore structure for excellent bone formation.
3. Bone formation and absorption of material: TCP-S bone formation generated more quickly than the absorption of materials in the earlier stage in the test of rat. TCP-S has a good balance with bone formation and material absorption.

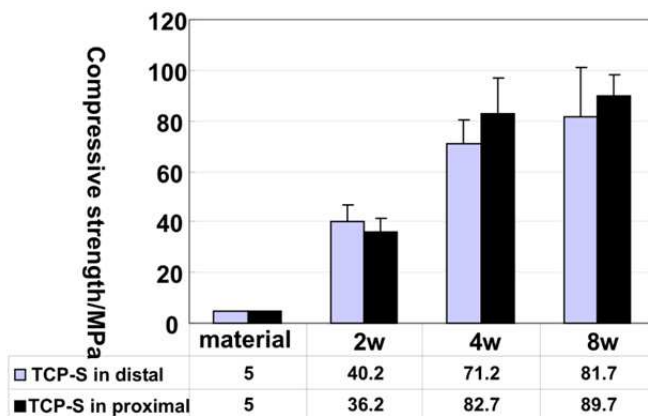


Fig. 12. Results of Compressive strength of TCP-S after implanted. During 4 and 8 weeks postoperatively, the compressive strength increased approximately 16 times more than that of the material only. The compressive strength of TCP-S implanted in defect bone was much higher than the material strength in the early stage.

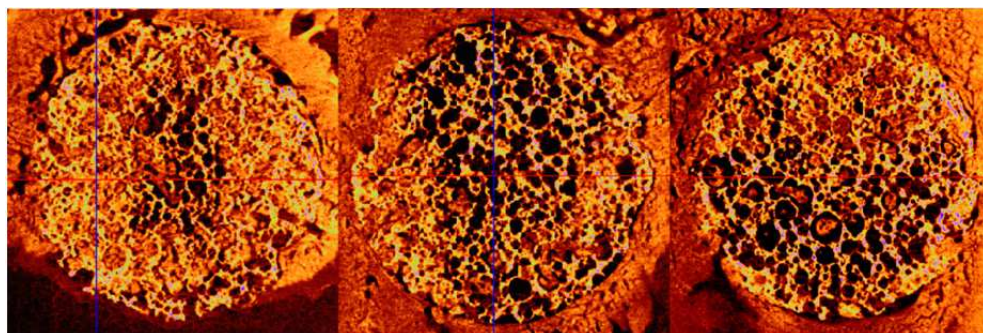


Fig. 13. Micro-CT image of calvaria of rat at after 4weeks implanted. Excellent bone formation in the TCP-S pellet was exhibited from the surroundings of the original bone.

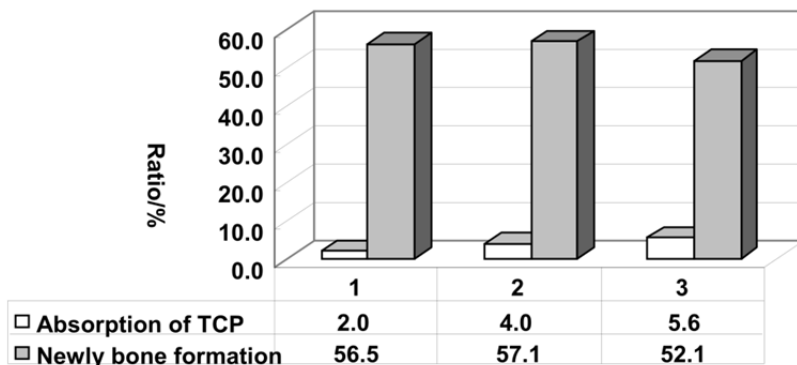


Fig. 14. Micro-CT analysis of TCP-S pellet at after 4 weeks implanted. The ratio of bone formation was 56.5%, 57.1% and 52.1% in implantation at 4 weeks. In addition, the absorption of TCP materials was mean 3.9% with the ratio of absorbent material TCP-S. In the results of rat, at 4 weeks after implantation, the ratio of new bone formation in the TCP-S was higher than the materials absorption.

9. Summary and conclusion

We developed porous beta-TCP ceramics (TCP-S) with a controlled triple pore structure, namely macro pores, interconnecting pores and micro pores. TCP-S showed good osteogenesis, bioresorption and recovery of strength in the early stage after implantation. TCP-S is useful for bone graft materials. In 2010, TCP-S (SUPERPORE, HOYA Co., Tokyo, Japan) was approved by the MHLW as a bone substitute in orthopedics. The clinical data on the follow-up more than 1 year after the treatment with TCP-S showed favorable results in all cases.

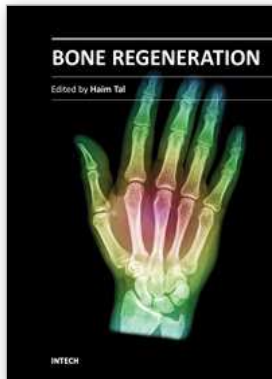
The triple pore structure with a macropore of 50~300 μm , an interconnecting pore of 50~100 μm , and a micro-pore of 0.5~10 μm showed strength recovery in osteoplasty at an early stage of the filling region without being affected by the composition of the artificial bone and it was the most suitable bone filling material.

10. References

- A.Myoi, H.Yoshikawa,.(2009),Clinical issues of bone substitutes,*J Jpn Orthop Assoc*,83, 463-468
- I.Ono et.al.,(2004),Studies on the dynamics of bone formation in porous hydroxyapatite ceramic.*The 13th Research Council Meeting of Japan Society of Plastic and Reconstructive Surgery*,Vol.13,p61
- M.Kato et.al.,(2006),Lumbar posterolateral fusion with beta-tricalcium phosphate,*The Central Japan Association of Orthopaedic Surgery & Traumatology*,49(6),1063-1064
- M.Motomiya, K.Kadoya, M.Ito, et.al.,(2006),The Potentiality of novel high porous hydroxyapatite for better spinal arthrodesis. *The Orthopaedic Research Society*,#p.875

- M.Motomiya, M.Ito, M.Takahata,et.al.,(2007),Effect of hydroxyapatite porous characteristics on healing outcomes in rabbit posterolateral spinal fusion model. *Eur Spine J.* 16,2215-2224.
- M.Motomiya,K.Kadoya,M.Ito et.al.,(2005),The effect of the presence or absence of bone union interconnecting pore and porosity of hydroxyapatite., *J.Jpn.Orthop*,Vol.79, No.8,S918
- M.Nakasu,H.Okihana,M.Sakamoto et.al.,(2005),Bone Formation of Highly Porous Hydroxyapatite with Different Pore Size Ranges,*CERAMICS JAPAN*,Vol.40, No.10, 828-830
- M.Ogiso,(2003),Titanium and apatite as implant materials,*Japanese Society for Biomaterial*,Vol.21,No.6,450-456
- M.Ogiso,S.Mineno,T.Matsumoto,(2004),Osteoanagenesis method that uses super-minute bone dust and porous apatite. Bone regeneration method using microscopic bone powder and porous apatite. *J.Jpn.Orthop.*,Vol.78,No.8,S799
- M.Ozawa et.al.,(2003/2004),Appropriate use of β -TCP.*Orthopaedic Ceramic Implants*,Vol 23/24,47-50
- M.Sakamoto et.al.,(2006),Biomechanical evaluation of ultra porous hydroxyapatite ceramics on in vivo study.*20thEuropean Conference on Biomaterials*,T54
- M.Sakamoto et.al.,(2008),Evaluation of porous beta-TCP ceramics with triple pore structure as bone tissue scaffold, *Orthopaedic Ceramic Implants*,Vol.28.5-8
- M.Sakamoto et.al.,(2009),Development and evaluation of porous Beta- TCP ceramics with triple pore structure. *The Orthopaedic Research Society*, #p.1376
- M.Sakamoto, M.Nakasu, T.Matsumoto et al.,(2007),Development of superporous hydroxyapatite and their examination with a culture of primary rat osteoblasts.*J Biomed Mater Res*, 82A, 238-242
- M.Sakamoto, T.Matsumoto, M.Nakasu et al.,(2005),Development and evaluation of porous hydroxyapatite ceramics with high porosity.*European Conference on Biomaterials*,No.19,p43
- M.Sakamoto,T.Matsumoto,M.Nakasu et.al.,(2004),Evaluation of porous Hydroxyapatite ceramics with high porosity as bone tissue scaffold,*The 24th Annual Meeting of The Japanese Society of Orthopaedic Ceramics and Implants*,Vol.24,p34
- M.Sakamoto,T.Matsumoto,T.Nakajima et.al.,(2006),Functional evaluation of porous hydroxyapatite bone regeneration using ultra-high porosity ceramics,*The Japanese Society for Regenerative Medicine*, Vol.5, No.19, p214.
- M.Takahata, M.Ito, M.Motomiya et al.,(2006),A novel technique to generate autogenous graft bone using ultra-high porous hydroxyapatite scaffold on in vivo ilium in preparation for spinal interbody fusion. *The Orthopaedic Research Society*,#p.1731
- N.Okii, S.Nishimura, K.Kurisu et al.,(2001),In vivo Histological Changes Occurring in Hydroxyapatite Cranial Reconstruction -Case Report-,*Neurologia Med Chir (Tokyo)*,41,100-104
- N.Yamazaki, M.Hirano, K.Nanno et al., (2009),A Comparative Assessment of Synthetic Ceramic Bone Substitutes With Different Composition and Microstructure in Rabbit Femoral Condyle Model,*J Biomed Mater Res Part B*, 91B, 788-798,

- S.Hirabayashi,K.Kumano,(1999),Contact of hydroxyapatite spacers with split spinous processes in double-door laminoplasty for cervical myelopathy,*J Orthop Sci* 4, 264-268
- T.Matsumoto,(2006),”Hoc nunc os ex ossibus meis”., *Japanese Society for Biomaterial*, Vol.24,No.1,39-40,2006
- T.Matsumoto,M.Sakamoto et.al.,(2004),Pore structure of high-porous hydroxyapatite ceramics. *The Society of Inorganic materials,JAPAN*,Vol.108th,p46
- T.Nakajima, et al.,(2010),In vivo histological study of posterolateral spinal fusion using superporous hydroxyapatites as a bone graft extender,*The 39th Annual Meeting of the Japanese Society for Spine Surgery and Related Research*,Vol.1,No.4,949
- T.Ueno, A.Ota, N.Shirasu et al.,(2009),A case of usage ultra-high porous hydroxyapatite for alveolar bone augmentation,*J Okayama Dental Soc*,28,65-69



Bone Regeneration

Edited by Prof. Haim Tal

ISBN 978-953-51-0487-2

Hard cover, 340 pages

Publisher InTech

Published online 04, April, 2012

Published in print edition April, 2012

Bone is a specialized connective tissue, most prominently characterized by its mineralized organic matrix that imparts the physical properties that allow bone tissue to resist load, to support functional organs, and to protect highly sensitive body parts. Bone loss and bone damage may occur as a result of genetic conditions, infectious diseases, tumours, and trauma. Bone healing and repair, involves integrative activity of native tissues and living cells, and lends itself to the incorporation of naturally derived or biocompatible synthetic scaffolds, aimed at replacing missing or damaged osseous tissues. There are several modalities of bone regeneration including tissue engineering, guided bone regeneration, distraction ontogenesis, and bone grafting. This book concentrates on such procedures that may well be counted among the recent outstanding breakthroughs in bone regenerative therapy.

How to reference

In order to correctly reference this scholarly work, feel free to copy and paste the following:

Michiko Sakamoto and Toshio Matsumoto (2012). Development and Evaluation of Superporous Ceramics Bone Tissue Scaffold Materials with Triple Pore Structure A) Hydroxyapatite, B) Beta-Tricalcium Phosphate, Bone Regeneration, Prof. Haim Tal (Ed.), ISBN: 978-953-51-0487-2, InTech, Available from: <http://www.intechopen.com/books/bone-regeneration/development-and-evaluation-of-superporous-ceramics-bone-tissue-scaffold-materials-with-triple-pore-s>

INTECH
open science | open minds

InTech Europe

University Campus STeP Ri
Slavka Krautzeka 83/A
51000 Rijeka, Croatia
Phone: +385 (51) 770 447
Fax: +385 (51) 686 166
www.intechopen.com

InTech China

Unit 405, Office Block, Hotel Equatorial Shanghai
No.65, Yan An Road (West), Shanghai, 200040, China
中国上海市延安西路65号上海国际贵都大饭店办公楼405单元
Phone: +86-21-62489820
Fax: +86-21-62489821

© 2012 The Author(s). Licensee IntechOpen. This is an open access article distributed under the terms of the [Creative Commons Attribution 3.0 License](#), which permits unrestricted use, distribution, and reproduction in any medium, provided the original work is properly cited.